(6) As with all spatially resonant systems, the injected beam must be well collimated;

(7) The perturbations should not be appreciably disturbed by the plasmas, so long as $2\mu_0 nkT/B_0^2 \ll 1$; but space charge will affect the energy of injected ions, and some allowance will have to be made in the injection energy. Reference 6 shows that even with large plasma diamagnetism, the trapping effect still exists;

(8) Resonant systems for other applications (e.g., injection into a torus) seem at least conceivable.

Regarding the loss of already trapped particles, an analysis has been given in Sec. IV that is applicable to a wide variety of perturbed systems. Equation (33) shows the importance of keeping the perturbation field $\tilde{B}$ (or $\tilde{\omega}_\perp$) no larger than required to achieve its desired purpose. For a given configuration, the confinement time $\propto 1/\tilde{B}^2$. Section V applies equally well to a resonant periodic mirror as to our case of a helically perturbed system.

Section VI shows that a helically perturbed system of the sort described here is not suitable for longtime trapping of the injected particles, because of the "resonance" diffusion described by Eq. (58). This difficulty is probably inherent in other resonant perturbation schemes, unless the trapped particles seldom encounter the perturbation region. The interesting possibility of effecting such a partial separation, for example by injection off axis into an azimuthally asymmetric structure, has not been investigated. Other nonresonant particles, formed for example by dissociation of the injected beam, are virtually unaffected by the perturbation, and their confinement time is set by other mechanisms.

ACKNOWLEDGMENTS

This work was supported in part by the U. S. Army Signal Corps, the U. S. Air Force Office of Scientific Research, and the U. S. Office of Naval Research; and in part by the National Science Foundation (Grant G-24073).

THE PHYSICS OF FLUIDS VOLUME 7, NUMBER 9 SEPTEMBER 1964

Orbit Stability in a Helically Perturbed Magnetic Field

L. M. LIDSKY

Department of Nuclear Engineering and Research Laboratory of Electronics, Massachusetts Institute of Technology, Cambridge, Massachusetts

(Received 29 November 1963)

The stability of particle orbits in resonant helices ("corkscrews") is investigated for axial acceleration and deceleration of the injected particles. It is shown that deviations from the unperturbed orbit lead to growing oscillations about that orbit for a decelerating corkscrew. The growth rate is small in devices suitable for injection into mirror fields. The numerical results are in agreement with experimental observations of injection parameters and output properties. Deviations from the equilibrium orbit in an accelerating corkscrew lead to damped oscillations.

I. INTRODUCTION

THE resonant transfer of longitudinal to transverse kinetic energy in a helically perturbed magnetic field ("corkscrew") has been demonstrated experimentally by Wingerson[1] and Dreicer, *et al.*,[2] and discussed in detail by Wingerson, Dupree, and Rose.[3] It has been shown that this resonance is stable to first order; that is, a particle displaced from the stable orbit will oscillate about the position of stability. We address ourselves here to the question of second-order stability: does an oscillation about the stable orbit grow or decay?

II. LINEARIZED EQUATIONS OF MOTION

For the coordinate system of Fig. 1, the orbital equations for $v_\perp$, the aximuthal velocity, and χ, the azimuthal angle between the particle position and the maximum of the helical field, are[4]

$$dv_\perp/dz = \omega_r(r, z) \cos \chi, \tag{1}$$

[1] R. C. Wingerson, Phys. Rev. Letters **6**, 446 (1961).

[2] H. Dreicer, H. J. Karr, E. A. Knapp, J. A. Phillips, E. J. Stovall, Jr., and J. L. Tuck, Nucl. Fusion Suppl. Pt. 1, 299 (1962).

[3] R. C. Wingerson, T. H. Dupree, and D. J. Rose, Phys. Fluids **7**, 1475 (1964).

[4] The notation differs slightly from that of Wingerson, Dupree, and Rose. In particular, the direction of positive magnetic field in this paper is opposite in sign to that chosen by Wingerson, Dupree, and Rose. This simplifies the equations discussed here.

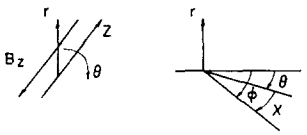

FIG. 1. Coordinate system for derivation of the orbital equations; θ is the angular position of the field maximum and ϕ is the angular position of the particle.

$$d\chi/dz = -2\pi/P(z) + \omega_z/[U - v_\perp^2]^{\frac{1}{2}}, \quad (2)$$

where $\omega_r = qB_r/m$, $\omega_z = qB_z/m$, $U = 2E_0/m$, E_0 is the total energy of the particle, and $P(z)$ is the local pitch length. As in Ref. 3, the assumption is made that the radial velocity, but not the radial position, can be ignored. If $v = v_0 + v_1$ and $\chi = \chi_0 + \chi_1$, where $v_0(z)$ and $\chi_0(z)$ refer to the unperturbed variable pitch helical orbit of the particle, then to first order in the perturbation variables χ_1 and v_1,

$$dv_1/dz = -\omega_r(r, z) \sin \chi_0 \chi_1, \quad (3)$$

$$d\chi_1/dz = +\omega_z v_0 v_1/[U - v_0^2]^{\frac{1}{2}}. \quad (4)$$

Equations (3) and (4) yield a second-order differential equation for χ_1, the angular displacement from the equilibrium orbit,

$$d^2\chi_1/dz^2 + g(z)\, d\chi_1/dz + h(z)\chi_1 = 0, \quad (5)$$

where

$$g(z) = \frac{3}{P(z)}\frac{dP(z)}{dz} - \frac{1}{v_0}\frac{dv_0}{dz} \quad (6)$$

and

$$h(z) = [(2\pi)^3 v_0(z)\omega_r(r, z) \sin \chi_0]/\omega_z^2 P^3(z). \quad (7)$$

It is easy to verify that some of the possible corkscrew orbits exhibit oscillatory stability. Consider a particle undergoing axial deceleration in a resonant helix. The perturbing field is a simple cosine function of azimuth at any fixed z with the position of the field maximum ($\theta = 0$) rotating in spatial synchronism with the orbit of the unperturbed particle. A particle in the first quadrant displaced forward in angle ($\chi_1 > 0$) is decelerated less strongly than a particle in the equilibrium orbit. The helix traced out by the displaced particle thus has a longer pitch (slower rotation in the frame moving with the equilibrium axial velocity) and χ_1 will decrease. Similarly, a particle displaced backward in angle moves with too small an axial velocity, tracing out an orbit of smaller pitch than that of the equilibrium particle and will move toward the equilibrium orbit. Analogous arguments can be made for perturbations in energy and, for the proper choice of operating quadrant, perturbations in an accelerating corkscrew.

Equation (5) is the linearized description of these oscillations. For a decelerating corkscrew, $dv_\perp/dz$ must be positive. To achieve the oscillatory behavior discussed above, $h(z)$ must be positive. Equations (1) and (2) thus allow first order stability only for $\omega_r > 0$ and $0 < \chi_0 < \frac{1}{2}\pi$. Similar considerations show that the stable orbit for an accelerating corkscrew must lie in the second quadrant. The growth or decay of the oscillations described by Eq. (5) depends on the sign of $g(z)$. For deceleration, $dv_\perp/dz > 0$ and $dP/dz < 0$ (the pitch decreases as the particle slows). Therefore, $g(z)$ is negative for any decelerating corkscrew and oscillations about the equilibrium orbit grow along that orbit. Conversely, the oscillations are damped in an accelerating corkscrew.

The magnitudes of $g(z)$ and $h(z)$ change as the particle moves along its orbit. The exact description of the oscillations thus requires that we specify the systems of interest. This is done, without linearization, in the following section.

III. OPTIMUM CORKSCREW

In Ref. 3 it is demonstrated that the scattering losses for trapped particles are reduced for a corkscrew in which $dv_\perp/dz \to 0$ at both ends. We consider first-pass particle motions in such a system. Particularly, we demand that the perpendicular velocity in the unperturbed orbit, $v_{\perp 0}$, be given by

$$v_{\perp 0} = \alpha v_0 \sin^2 (\pi z/2L), \quad (8)$$

where α is a parameter describing the total change in perpendicular velocity, v_0 is the speed of the particle, and the corkscrew length is L. The resonance condition gives

$$P(z) = (2\pi v_0/\omega_z)[1 - \alpha^2 \sin^4 (\pi z/2L)]^{\frac{1}{2}} \quad (9a)$$

$$= P_0[1 - \alpha^2 \sin^4 (\pi z/2L)]^{\frac{1}{2}}. \quad (9b)$$

Equations (1), (8), and (9b) combine to fix the necessary variation of $\omega_r(r, t)$:

$$\omega_r(r, z) = \frac{(\pi\alpha/2L) \sin (\pi z/L)}{G(\chi_0, z) \cos \chi_0} \cdot \left\{ I_0\left[\frac{2\pi r}{P(z)}\right] + I_2\left[\frac{2\pi r}{P(z)}\right] \right\}, \quad (10)$$

where[5]

$$G(r_0, z) = G\left(\frac{v_{\perp 0}}{\omega_z}, z\right) = I_0\left[\frac{2\pi v_{\perp 0}(z)}{\omega_z P(z)}\right] + I_2\left[\frac{2\pi v_{\perp 0}(z)}{\omega_z P(z)}\right]. \quad (11)$$

[5] The magnetic field of a set of helical conductors is derived in Ref. 3, Sec. II.

The algebra is simplified by introducing the new variables $x = \pi z/2L$, $v = v_\perp/v_0$, and $p(x) = P(x)/P_0$. In this notation,

$$\frac{dv}{dx} = \frac{\alpha \sin 2x}{G(v_{\perp 0}, x) \cos \chi_0} G(v, x) \cos \chi \qquad (12)$$

and

$$\frac{d\chi}{dx} = \frac{4L}{P_0}\left[\frac{1}{(1 - v^2)^{\frac{1}{2}}} - \frac{1}{p(x)}\right]. \qquad (13)$$

We take advantage of the fact that the unperturbed orbit is known and rewrite the equations in terms of deviations from this orbit; that is, for $\chi_1(x) = \chi(x) - \chi_0$ and $v_1(x) = v(x) - v_0(x)$. These equations are

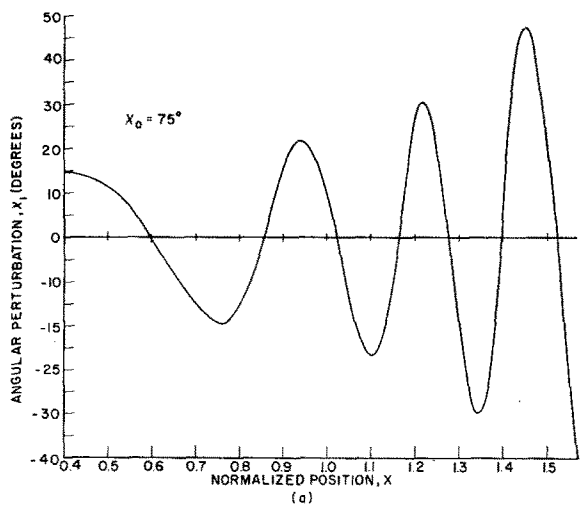

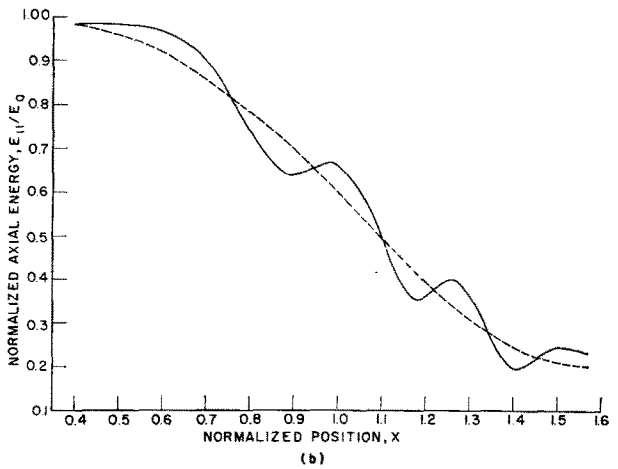

FIG. 2. (a) Angular deviation of particle position from the equilibrium orbit as a function of the normalized distance x. $x = \pi z/2L$, where z is the position of the particle, and L is the length of the helical field. (b) Normalized z-directed energy of the particle as a function of x. The dashed line illustrates the behavior of an unperturbed particle.

$$\frac{dv_1}{dx} = \alpha \sin 2x \cdot\left\{\frac{G(v_0 + v_1, x)}{G(v_0, x)} (\cos \chi_1 - \tan \chi_0 \sin \chi_1) - 1\right\} \qquad (14)$$

$$\frac{d\chi_1}{dx} = \frac{\Lambda}{p(x)}\left\{\frac{1}{1 - [(2\alpha \sin^2 x v_1 + v_1^2)/p^2(x)]^{\frac{1}{2}}} - 1\right\}, \qquad (15)$$

where

$$p(x) = [1 - \alpha^2 \sin^4 (x)]^{\frac{1}{2}}, \qquad (16)$$

$$G(v_0 + v_1, x) = I_0\left[\frac{\alpha \sin^2 (x) + v_1}{p(x)}\right] + I_2\left[\frac{\alpha \sin^2 (x) + v_1}{p(x)}\right], \qquad (17)$$

and

$$\Lambda = 4L/P_0. \qquad (18)$$

Except for the slowly varying ratio of the G's, Eqs. (14) and (15) are first order in deviations from equilibrium. The oscillations about the unperturbed orbit are thus separated from the equations of the orbit itself, and can be studied with far greater accuracy. Notice also that no additional approximations have been made (that is, these equations are not linearized.)

Equations (14) and (15) were solved numerically by four-step Runge–Kutta integration. The results presented below were all computed by using a normalized distance increment of 10^{-3} (1570 steps for a single traverse). The results at the end of a complete pass were changed at most by 2 parts in the fifth significant figure for distance increments of 10^{-2} and 10^{-4}.

IV. NUMERICAL RESULTS

The equations of the system are characterized by three parameters: α, the ratio of exit azimuthal velocity to the total velocity of the particle; Λ, a number of proportional to the number of "corkscrew turns" in the system ($\Lambda = 4L/P_0$); and χ_0, the particle phase for which the corkscrew was designed.

Numerical computations were carried out for systems comparable to the electron corkscrew experiments of Wingerson and Dreicer ($\Lambda = 20$) and for the more finely tuned systems of ultimate interest. We considered α values of 0.500 and 0.894 (25 and 80% of the energy in transverse motion at the exit), Λ values of 50 and 100, and design angles of 30°, 45°, 75°, and ±135°. The last two values are for the stable and unstable quadrants

for an accelerating corkscrew ($\frac{1}{2}\pi \leq x \leq \pi$). The Λ values are those of an electron corkscrew with for example, 200 G main axial field, 1600 V injection energy, and 53 ($\Lambda = 50$) or 106 cm ($\Lambda = 100$) length. The number of turns depends in part on the value of α. For $\alpha = 0.894$ and $\Lambda = 100$, this number is approximately 52. Some typical results are discussed below for this last case.

A. Decelerating Corkscrews

A corkscrew as defined by Eq. (9) is decelerating for $0 \leq x \leq \frac{1}{2}\pi$, and is phase stable for χ_0 in the first quadrant. Figure 2(a) shows the effect of a 15° perturbation in the angular position at $x = 0.4$. As expected, the oscillations grow in magnitude and frequency along the corkscrew. Figure 2(b) is a plot of axial energy during these oscillations compared with the smooth deceleration of an unperturbed particle. The angular-position perturbation leads to an energy perturbation because a particle in the first quadrant displaced forward in χ is subject to a smaller radial field, and is decelerated less strongly than an unperturbed particle.

Figure 3 illustrates the effect of an energy perturbation ($\Delta E = -0.06$) at the same position. The phase angle χ at various axial positions is marked off along the curve. The particle was lost when χ become more negative than $-45°$ at a time when the axial velocity was higher than the axial velocity for an unperturbed particle. The radial field for $\chi < -45°$ is smaller than the design field, and the particle slipped even farther behind in phase. The radial field is negative for $-\frac{3}{2}\pi \leq \chi \leq \frac{1}{2}\pi$, and the particle was accelerated. It continued to slip behind in phase because $d\phi/dz = (1/v_z)\, d\phi/dt$ was everywhere smaller than $d\theta/dz$ as defined by the corkscrew windings. Successive cycles of acceleration and deceleration followed, but the effect of each

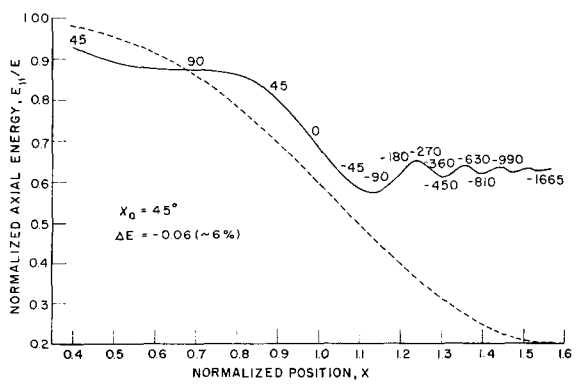

FIG. 3. Normalized z-directed energy vs x. The particle phase χ is plotted as a running parameter.

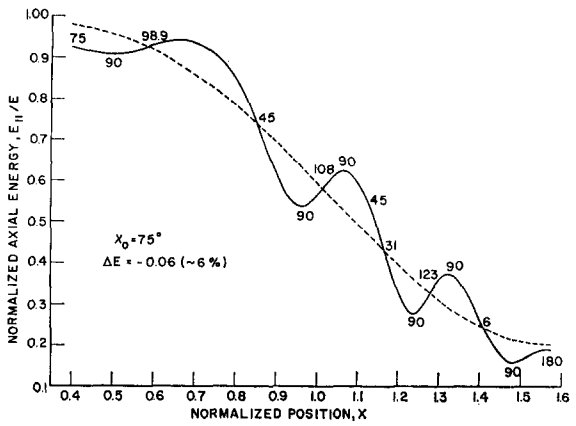

FIG. 4. Normalized z-directed energy vs x. The conditions for this case differ from those of Fig. 3 only in the value of χ_0. χ is the running parameter.

became smaller because the particle spent less time in the successively shorter sections. This latter motion is an example of the nonresonant "random" perturbations described in Ref. 3.

Figure 4 is a plot of the same case for an initial design phase χ_0 of 75°. Two factors cause this situation to be more stable than that in Fig. 3. First, the particle must slip farther back in phase to see a radial field weaker than the design field. Second, and more important, the ratio of maximum radial field to design field is larger for $\chi_0 = 75°$ than it is for $\chi_0 = 45°$. [$\omega_r(\chi = 0°) = 1.4\omega_r(45°) = 3.9\omega_r(75°)$]. The improved stability is of course accompanied by increased perturbation of previously trapped particles.

Note that although the equilibrium orbit is stable only in a single quadrant for any given corkscrew, the orbit of the perturbed particle may pass through three quadrants while still oscillating about the unperturbed orbit. Thus, in Fig. 4 for example, the axially accelerating field in the second quadrant serves to move the too slowly moving particle at $x = 1.05$ toward the proper orbit.

B. Accelerating Corkscrews

The pitch equation (9) describes an accelerating corkscrew for $\frac{1}{2}\pi \leq x \leq \pi$. A system with parameters identical to the decelerating corkscrew discussed above ($\alpha = 0.894$, $\lambda = 100$) was investigated for the case $\chi_0 = 135°$ and $x > \frac{1}{2}\pi$. The effect of an angular perturbation at the entrance is depicted in Fig. 5. The result of an identical perturbation for a particle in the unstable accelerating quadrant ($\chi_0 = -135°$) is shown. As predicted, the oscillations of the particle in the proper quadrant are rapidly damped. The angular oscillations resulting from a

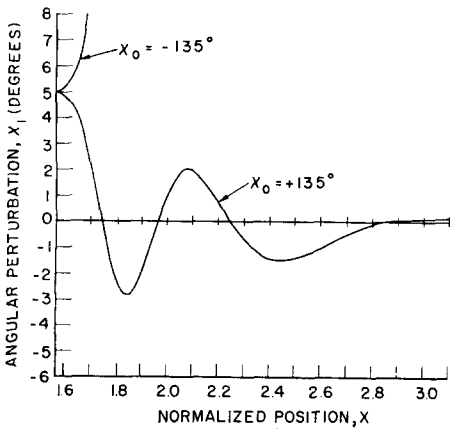

FIG. 5. Angular deviation vs x for an accelerating corkscrew. Note that $\frac{1}{2}\pi \leq x \leq \pi$ for this case.

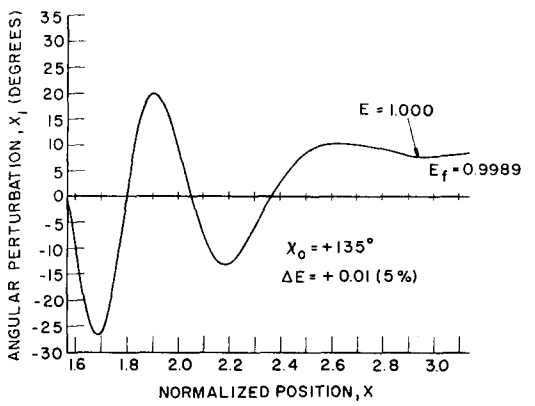

FIG. 6. Angular deviation vs x for the corkscrew of Fig. 5. In this case, the initial perturbation was in energy.

5% energy perturbation at the entrance are shown in Fig. 6. The particle was completely unwound at the local minimum at $x = 2.95$. The longitudinal energy at the exit was 0.9989 of the total energy.

V. CONCLUSIONS

The numerical results presented for the decelerating corkscrew show the presence of the growing oscillations predicted by the linearized theory, and further demonstrate that the growth rate is small for most systems of interest. The numerical results agree with the experimental work of Dreicer and his co-workers[2] in showing that a small energy spread at the exit is accompanied by a large spread in exit phase. The size of the "acceptance hole" at the corkscrew entrance is also in agreement with experiment ($\pm \sim 10\%$ in energy, $\pm \sim 30°$ in phase).

Figure 3 indicates that particles can be partially wound up to an extent determined by their initial deviation from the stable orbit. This calls into question the intuitive conclusion that the optimum system would consist of a finely tuned corkscrew with a very carefully matched injection system. It is likely that an injection system with a moderate spread in particle velocity (resulting in a wide spread in energy and phase at the corkscrew exit) would circumvent many of the difficulties that plague devices with highly ordered particle motions.

This accelerating corkscrew presents intriguing possibilities for injection into "closed" toroidal systems. In the simple form discussed in this report it is capable of placing particles on the axis of a toroidal system whose minor radius is equal to the cyclotron radius of a particle with total velocity in the transverse direction. Injection into a field extending over several cyclotron radii is more desirable.

ACKNOWLEDGMENTS

Numerical computations were performed at the Massachusetts Institute of Technology Computation Center.

This work was supported in part by the U.S. Army Signal Corps, the Air Force Office of Scientific Research, and the Office of Naval Research; and in part by the National Science Foundation (Grant G-24073).